

dry hexane cooled to -78°C was slowly added 15 ml (30 mmol) of 2.0M *t*-butyllithium in pentane. The mixture was allowed to warm slowly to room temperature and was stirred overnight. Work-up as described above was followed by GC analysis which gave 74% yield of 1-methoxy-1,1-diphenyl-2-trimethylsilyl-4,4-dimethyl-1-silapentane. This product was isolated by column chromatography as colorless liquid.

1-Methoxy-1,1-diphenyl-2-trimethylsilyl-4,4-dimethyl-1-silapentane 5; colorless liquid; $^1\text{H-NMR}$; δ -0.09(s, 9H, $-\text{Si}(\text{CH}_3)_3$), -0.03-0.45(m, 1H, Si-CH-Si), 0.75(s, 9H $-\text{C}(\text{CH}_3)_3$), 1.2-1.6 (m, 2H, $-\text{CH}_2-$), 3.55(s, 3H, $-\text{OCH}_3$), 7.2-7.8(m, 10H, Si-aryl); $^{13}\text{C-NMR}$, δ 0.60, $-\text{Si}(\text{CH}_3)_3$; 8.11, Si-CH-Si; 29.62, $-\text{C}(\text{CH}_3)_3$; 31.77, $-\text{C}(\text{CH}_3)_3$; 37.35, $-\text{CH}_2-$; 51.45, $-\text{OCH}_3$; 127.71, 127.99, 129.49, 135.29, 135.34, 135.86; 136.44, Si-aryl; MS; m/z (relative intensity), $[\text{M}^+ - 15]$ 355(82), 313(34), 213(100), 209(8), 106(5), 73(22), 59(20), 57(7).

Trapping reaction with anthracene. To a mixture of 4.9 g(20 mmol) of chlorodiphenylvinylsilane and 6.41 g (36 mmol) of anthracene in 700 ml of dry benzene at room temperature was slowly added 10 ml (20 mmol) of 2.0 M *t*-butyllithium in pentane. The mixture was allowed to stir overnight and then subjected to the usual work-up. GC analysis showed the mixture of dimers in 21% and the expected trapped adduct, 2,2-diphenyl-3-neopentyl-(5,6:7,8)-dibenzo-2-silabicyclo-(2.2.2)-octane, in 46%. The dimeric isomers were precipitated out from the product mixture in hexane at low temperature (ca. 0°C). The remaining solution was applied to a liquid chromatographic column to get the pure anthracene adduct (mp 165-166 $^{\circ}\text{C}$, colorless crystal).

2,2-Diphenyl-3-neopentyl-(5,6:7,8)-dibenzo-2-silabicyclo-(2.2.2)-octane, 6; colorless crystal; $^1\text{H-NMR}$, δ 0.86(s, 9H, $-\text{C}(\text{CH}_3)_3$), 1.23(d, 2H, $-\text{CH}_2-$), 1.42-1.80(m, 1H, Si-CH-NP), 4.31(s, 1H, Si-CH=), 4.45(d, 1H, $-\text{CH}=\text{}$), 6.68-7.56(m, 18H, aryl); $^{13}\text{C-NMR}$, δ 23.80, Si-CH-NP; 29.90, $-\text{C}(\text{CH}_3)_3$; 32.32, $-\text{C}(\text{CH}_3)_3$; 40.21, Si-CH=; 43.15, $-\text{CH}_2-$; 53.20, $-\text{CH}=\text{}$; 124.27, 124.93, 125.07, 125.57, 125.58, 126.07, 126.19, 126.89, 127.22, 127.53, 129.16, 129.24, 133.15, 134.16, 135.06, 136.55, 139.81, 140.07, 141.24, 142.71, phenyl car-

bons. MS; m/z (relative intensity), $[\text{M}^+]$ 444(3), 266(21), 210(20), 209(100), 184(5), 183(30), 178(13), 105(10), Anal.; Calcd. for $\text{SiC}_{32}\text{H}_{32}$; C, 86.42; H, 7.27 Found; C, 86.62; H, 7.35

Acknowledgement. We are grateful to the Korea Science and Engineering Foundation for financial support and also to Professor Wan Chul Joo of Sung Kyun Kwan University for help in obtaining $^{13}\text{C-NMR}$ spectra.

References

1. Representative reviews: (a) G. Rabbe and J. Michl, *Chem. Rev.* **85**, 419-509 (1985); (b) N. Wiberg, *J. Organomet. Chem.*, **273**, 14-177 (1984); (c) G. Bertrand, G. Trinquer and P. Mazerolles, *J. Organomet. Chem. Lib.*, **12**, 1-52 (1981); (d) L. E. Gusel'nikov and N. S. Nametkin, *Chem. Rev.*, **79**, 529-577 (1979).
2. P. R. Jones and T. F. O. Lim, *J. Am. Chem. Soc.*, **99**, 2013, 8447 (1977).
3. N. Wiberg and G. Preiner, *Angew. Chem., Int. Ed. Engl.*, **16**, 328 (1977).
4. P. R. Jones and M. E. Lee, *J. Organomet. Chem.*, **232**, 33-39 (1982).
5. (a) P. R. Jones, T. F. O. Lim and R. A. Pierce, *J. Am. Chem. Soc.*, **102**, 4970 (1980); (b) P. R. Jones, M. E. Lee and L. T. Lim, *Organometallics*, **2**, 1039-42 (1983).
6. P. R. Wells and F. Franke, *J. Org. Chem.*, **44**, 244 (1979).
7. F. W. Wehrly and T. Wirthlin, "Interpretation of C-NMR Spectra", Heyden and Son, Ltd., London, 37-39 (1976).
8. P. Jonh, B. G. Gowenlock and P. Groome, *J. Chem. Soc., Chem. Commun.*, 806-7 (1981).
9. P. R. Jones, A. H-B. Cheng and T. E. Albanesi, *Organometallics*, **3**, 78-82 (1984).
10. (a) J. L. Luche and J. C. Damiano, *J. Am. Chem. Soc.*, **102**, 7926 (1980); (b) J. L. Luche, C. Petrier, A. L. Gemal and N. Zikra, *J. Org. Chem.*, **47**, 3806 (1982).

XPS Studies of Oxygen Adsorption on Polycrystalline Nickel Surface

Soon-Bo Lee, Jin-Hyo Boo, and Woon-Sun Ahn*

Department of Chemistry, Sung Kyun Kwan University, Suwon 170. Received May 14, 1987

The interaction of oxygen with polycrystalline nickel surface has been studied by investigating the X-ray photoelectron spectra of 0 1s, Ni 2p_{3/2}, and their valence band electrons. By comparing the oxygen exposure of this work with the reported results of LEED, AES, and work function measurements, it is found that the atomic oxygen, adsorbed dissociatively in the initial stage of exposure, is responsible for a p(2 × 2) structure and a subsequent c(2 × 2) structure on the Ni(100) surface. This dissociatively adsorbed oxygen species forms surface NiO layer subsequently on further oxygen exposure. The NiO layer is more easily formed with the increasing temperature. Non-stoichiometric oxygen species is also found to accompany the NiO layer. It appears prior to the formation of bulk NiO at all of the temperatures of this work except at 523K.

Introduction

There have been up to now quite a number of investiga-

tions of the oxygen adsorption on nickel surface¹⁻¹¹, as the subject is very crucial in understanding such surface processes, as oxidation, heterogeneous catalysis, and adsorption

mechanisms. According to LEED and AES studies reported so far^{1,2}, oxygen molecules are chemisorbed dissociatively from the initial stage of adsorption, and form a $p(2 \times 2)$ structure of 0.25 monolayer coverage on Ni(100) considerably rapidly. With the increasing oxygen exposure, the rate of adsorption decreases and the adsorbed layer shifts to a $c(2 \times 2)$ structure at the half monolayer coverage.

In XPS studies of oxygen species adsorbed on Ni(100) surface, Brundle *et al.*³⁻⁶ detected two $0\ 1s$ peaks at 529.5 eV (binding energy) and 531.4 eV. Referring to UPS and AES results, they have assigned the first peak to dissociatively adsorbed oxygen atoms as well as to the oxide atoms of NiO, and the latter peak to Ni_2O_3 type oxygen atoms, which, according to them, can be formed on surface defect sites. However, Norton *et al.*⁸ objected the assignment of the latter peak on the ground that the oxygen species in $Ni(OH)_2$, formed from residual H_2O gas in vacuum systems, occupies almost the same peak position. Brundle *et al.*⁶ observed also a third $0\ 1s$ peak at 533.2 eV in the submonolayer region at the low temperature of 77K. They assigned the peak to the chemisorbed oxygen species in a stage of precursor to the oxide species.

Fleisch *et al.*⁷ also investigated oxygen adsorption on Ni(100) with XPS, LEED, and SIMS, and found that the adsorption rate is very slow in the initial stage, and that the $p(2 \times 2)$ structure and the subsequent $c(2 \times 2)$ structure are formed at the oxygen exposure of 40L through 50L. At 300L, oxygen adsorbs in maximum amount, forming two molecular layers of NiO. They found a single peak of $0\ 1s$ at 530.1 ± 0.2 eV in the initial stage of the dissociative adsorption. However, they found two more $0\ 1s$ peaks at 529.7 eV and 531.3 eV over the half monolayer coverage, and assigned the former to NiO and the latter to Ni_2O_3 . As to the Ni $2p_{3/2}$ binding energy, they found that the initial Ni $2p_{3/2}$ peak at 852.8 eV decreases in intensity with the formation of NiO, while a new peak appears at 854.6 eV. XPS and UPS studies by Norton⁸ and Evans⁹ also show similar results in general.

Kim *et al.*^{10,11} also investigated the $0\ 1s$ binding energies of NiO_{ad} , NiO, Ni_2O_3 , $NiOO_{ad}$, and $Ni(OH)_2$. They found the $0\ 1s$ peak at 531.3 ± 0.4 eV decreasing with the increasing temperature, and assigned the peak to Ni_2O_3 . The $0\ 1s$ peak, they assigned to NiO_{ad} , appears at 533.1 ± 0.4 eV, which is a little bit higher than the value reported by Norton⁸, Evans⁹, and Fleisch.

As above, there are still divergent conclusions as to the details of the oxygen chemisorption on nickel, especially as to the surface species formed thereupon. In this work authors have assayed chemical species formed in the course of oxygen chemisorption systematically, by investigating the $0\ 1s$ and the Ni $2p_{3/2}$ and $3d$ XPS spectral regions at various temperatures between the room temperature through 523K.

Experimental

All the measurements are performed in the ultra high vacuum XPS system (ESCA 750, Shimadzu Co., Japan) on which a quadrupole mass spectrometer (VG. Ltd., Masstorr FX, England) is attached. The pressure of the ESCA chamber is kept below 4×10^{-9} Torr and monitored with a BA ionization gauge. Polycrystalline nickel of purity 99.9% (Fruchi Chem. Co., Japan) is used as the adsorbent, and carbon and oxygen which are the major surface contaminants

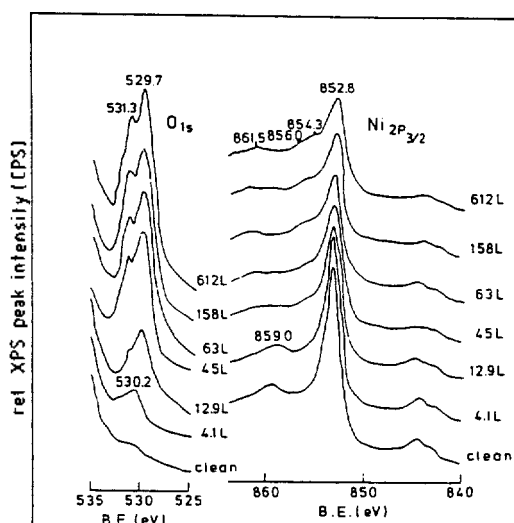


Figure 1. $O(1s)$ and $Ni(2p_{3/2})$ photoelectron spectra for varying oxygen exposure on polycrystalline nickel surface at 298K.

are eliminated by repeated processes of argon ion sputtering followed by oxidation with oxygen gas at high temperature. The surface damaged thereupon is regenerated by annealing at about 700K. The adsorbate oxygen gas (99.95% pure, Matheson Co., USA) is introduced through a variable leak valve at 10^{-7} through 10^{-8} Torr. A 1253.6 eV Mg K source is used, and the spectra are calibrated to Ag $3d_{5/2}$ (367.9 eV), Au $4f_{7/2}$ (83.8 eV), and Cu $2p_{3/2}$ (932.4 eV) peaks.

Results

In the present work, the XPS spectral regions of $0\ 1s$ (535-525 eV), Ni $2p_{3/2}$ (870-840 eV), and Ni valence band (30-0 eV) have been investigated at 298, 373, 423, and 523K.

(I) Spectra at 298K. The XPS spectra in the $0\ 1s$ and Ni $2p_{3/2}$ regions are shown in Figure 1 as a function of oxygen exposure at 298K. Up to 12.9L ($1L = 1 \times 10^{-6}$ Torr sec) exposure, the intensity of the $0\ 1s$ peak at 530.2 eV increases significantly, while those of the Ni $2p_{3/2}$ peak at 852.3 eV and the Ni $2p_{3/2}$ satellite peak at 859.0 eV do not change. The $0\ 1s$ peak at 530.2 eV is due to the atomic oxygen species. This atomic species is found to form a $p(2 \times 2)$ structure at first and then a $c(2 \times 2)$ structure of half monolayer coverage in accordance with AES and LEED studies.^{1,2} This interpretation is also supported by the previous XPS studies of single crystal Ni/oxygen systems.⁷⁻⁹ The kinetic and energetic explanation for this adsorption process will be presented in other paper.

On further oxygen exposure, the peak at 530.2 eV is replaced by steadily developing peaks at 531.3 and 529.7 eV. Beyond 63L exposure, however, the peak at 529.7 eV increases in intensity rapidly with the increasing oxygen exposure, while the other one at 531.3 eV remains unchanged. Meanwhile, both the Ni $2p_{3/2}$ peaks at 852.8 eV and 859.0 eV decrease with the simultaneous appearance of new peaks at 861.5, 856.0, and 854.3 eV. According to many others' previous works^{7-9,13-14}, the peaks at 529.7 and 854.3 eV are most probably due to NiO. However, as to the $0\ 1s$ peak at 531.3 eV and the Ni $2p_{3/2}$ peak at 856.0 eV, there are divergent opinions. For example, some^{7,10,11} attribute the peak to Ni_2O_3 ,

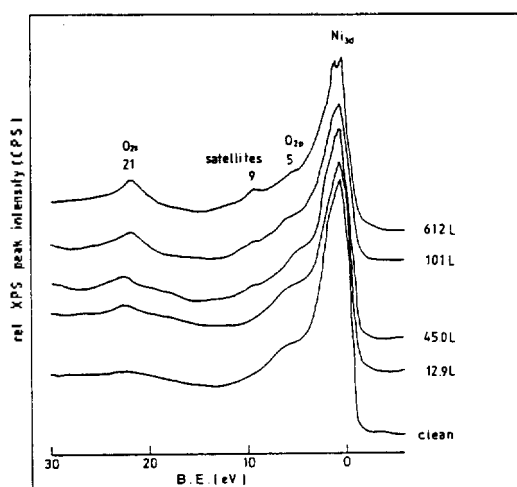


Figure 2. XPS valence band spectra for varying oxygen exposure on polycrystalline nickel surface at 298K.

which can, according to them, be formed on the defect sites of Ni surface, while others^{3,4,14} to NiO(H). As there remains always residual H₂O gas in the ESCA chamber, there is a possibility of NiO(H) species formation.

In order to ascertain these two peaks, about 10-15L of oxygen is dosed in this work, and then the peaks are monitored for the subsequent 12 hours at room temperature. Neither the binding energy changes nor the intensity changes have been observed. Therefore, it is concluded that the peaks are not due to the resultants of the residual H₂O molecules. Considering, in addition, that the Ni peak corresponds to a more highly oxidized state than NiO(854.3eV), and that the oxygen peak to a less reduced state than NiO(529.7eV), it is quite evident that the peaks result from the non-stoichiometric oxygen adsorption over the surface NiO layer. More detailed explanation will be given later in the discussions (III).

The XPS valence band spectra of the clean nickel surface show the Ni 3d peak clearly, as shown in Figure 2. The figure shows also a broad satellite peak at a little bit higher binding energy (about 7eV). This satellite peak is due to multi-electron excitation and plasmon losses.⁹ Up to 12.9L oxygen exposure, the intensity of Ni 3d peak is not affected as those of Ni 2p_{3/2} peaks. Over 12.9L exposure, new peaks appear at 21, 9, 5, and 2eV, and their intensities increase steadily with the increasing oxygen exposure. Meanwhile, the Ni 3d band decreases in intensity significantly, though its width increases. When the surface oxygen reaches the maximum coverage, the Ni 3d band peak splits to show a new peak at 2eV. The UPS studies by Eastman¹⁸, Norton⁸, and Evans⁹ show similar results but for intensities. In UPS, the 3d peak vanishes at this maximum coverage. The difference is believed to arise because deep 3d electrons together with surface 3d electrons can contribute to the 3d valence peak of XPS, as the escaping depth of XPS is much longer than that of UPS. Considering this 2eV peak in connection with the 0 1s and Ni 2p_{3/2} peaks, it is certain that the peak is due to Ni²⁺(d⁸). And a peak on the shoulder of 3d peak at about 5eV is certainly due to the oxygen 2p band. This assignments can be supported by theoretical works¹⁵⁻¹⁷ which show that the 2p oxygen level can couple with the Ni 3d band to form a 2p band of oxygen at about 5eV. Two peaks at 21 and 9eV coincide with the XPS valence band spectrum, obtained by G.K. Wer-

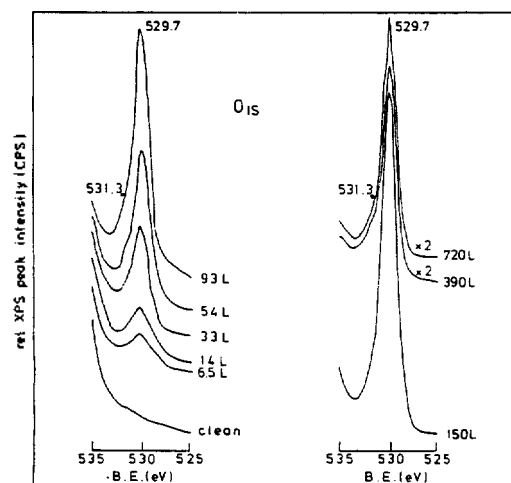


Figure 3. O(1s) photoelectron spectra for varying oxygen exposure on polycrystalline nickel surface at 523K.

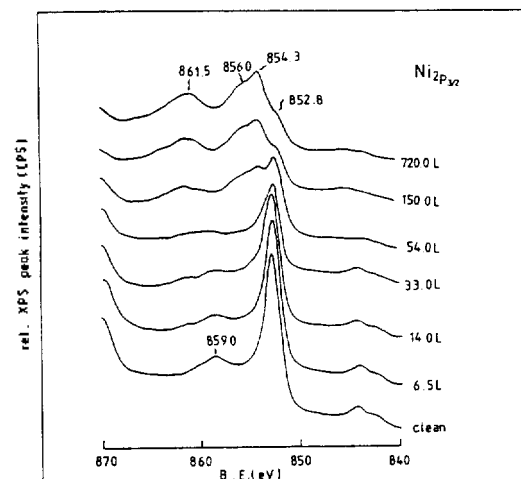


Figure 4. Ni(2p_{3/2}) photoelectron spectra for varying oxygen exposure on polycrystalline nickel surface at 523K.

them¹³ with NiO. He assigned the former peak to the 0 2s and the latter to a satellite peak shifted from 7eV.

(II) Spectra at 373 and 423K. The 0 1s spectra taken at 373 and 423K are quite similar to those taken at 298K. At the initial stage of adsorption, a peak appears at 530.2eV only, due to the dissociatively adsorbed oxygen species. With the increasing oxygen exposure two more peaks appear subsequently at 531.3 and 529.7eV. They appear at 23.0L exposure at 373K, and at 29.0L at 423K, while they have appeared at 12.9L at 298K. This suggests that the rate of dissociative adsorption decreases with the increasing temperature.

The intensity ratio of the peak at 531.3eV to the one at 529.7eV is found to decrease very clearly with the increasing temperature. This reflects the fact that the excess nonstoichiometric oxygen over the NiO structure becomes unstable thermodynamically, while NiO itself can be formed relatively easily to give a thicker NiO layer as the temperature rises. The Ni 2p_{3/2} peaks and the Ni valence band peaks at these two temperatures appear at the same binding energy positions of 298K. However, the intensities of Ni 2p_{3/2} peak at 852.8eV and the Ni 3d peak due to the pure nickel decrease

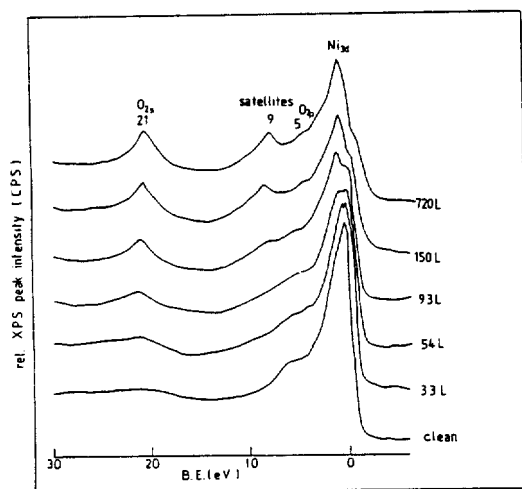


Figure 5. XPS valence band spectra for varying oxygen exposure on polycrystalline nickel surface at 523K.

significantly, while those of Ni $2p_{3/2}$ peak at 854.3eV and the Ni 3d peak at 2eV increase. Along with the behavior of the O 1s peaks, this temperature dependency of the nickel peaks are attributed to the thickening of the surface NiO layer.

(III) Spectra at 523K. The spectra of the O 1s and the Ni $2p_{3/2}$ at various oxygen exposures at 523K are shown in Figure 3 and 4, respectively. The O 1s peak at 530.2eV, due to the dissociatively adsorbed oxygen, appears no more at this temperature, while it has appeared consistently in the initial stage of adsorption throughout the lower temperatures. The O 1s peak at 529.7eV, however, appears persistently in all of the successive series of oxygen exposure up to the saturation. On the other hand, the Ni $2p_{3/2}$ spectra in Figure 4 show similar peak positions with those observed at the lower temperatures. However, their intensities show considerable changes; i.e., the peak at 852.8eV due to the pure Ni is decreased considerably at the saturation state, while the one at 854.3eV is increased eminently. The peak at 856.0eV due to the nonstoichiometric oxygen is still recognizable, though very weak near the saturation state. The above results as a whole suggest that the dissociatively adsorbed state oxygen is unstable at this temperature, and that oxygen forms NiO as soon as it is adsorbed. However, there might be a possibility, not sure enough, that the weak O 1s peak at 531.3eV due to the trace of nonstoichiometric excess oxygen, might be hidden unresolved under the intense 529.7eV peak.

Valence band spectra at various oxygen exposures at 523K are shown in Figure 5. The binding energies of the spectral peaks coincide with those taken at other temperatures. However, the 3d peak of pure nickel decreases significantly with the increasing oxygen exposure, and the peak at 2eV due to NiO increases considerably. These intensity changes are perfectly in accord with the fact that both the O 1s peak at 529.7eV and the Ni $2p_{3/2}$ peak at 854.3eV, due to NiO, increase in intensity, while the Ni $2p_{3/2}$ at 852.8eV due to pure Ni decreases. To sum up the above observations, it is certain that the interaction of oxygen with nickel surface results in NiO formation directly above 523K.

Discussions

(I) Dissociatively Adsorbed Oxygen. The O 1s peak which appears prior to the appearance of the 529.7eV peak at

298, 373, and 423K is believed as the one due to the rapidly adsorbed dissociative oxygen in the early exposure stage. This assignment differs somewhat from previously published ones. Earlier workers^{8,9} also observed ca. 0.5eV decrease of the O 1s binding energy when the dissociative adsorption shifts to NiO formation though, they have ascribed this to an energy drift accompanying the migration or rearrangement of surface atoms in the course of NiO formation.

When the oxygen exposures of this work at which various O 1s peaks formed are compared with the reported results of LEED,^{19,20} AES,^{1,2} and work function measurements,^{1,9} it is found that the dissociatively adsorbed oxygen species is responsible for the $p(2 \times 2)$ and $c(2 \times 2)$ structure of 0.25 and 0.5 coverage, respectively. A further support for this interpretation comes from the results of LEED intensity measurements^{19,20} and He-scattering¹⁵ which show that the oxygen species of these two structures have the same separation from the nickel surface. Moreover, according to the work function measurement reports^{1,9} these oxygen species are negatively polarized, but not to the extent of the ionized O^{2-} in NiO. This accounts for a bit higher binding energy of this O 1s electrons in comparison with those of NiO forming oxygen, and accordingly the peak at 530.2eV is assigned to the dissociatively adsorbed oxygen and the other peak at 529.7eV to the NiO forming oxygen. The XPS valence band spectra of this work and the UPS results^{8,9} also confirm these assignments. That is, the Ni 3d band is not perturbed at all throughout this work by the oxygen adsorption as far as the oxygen exposure is low enough that a O 1s peak appears at 530.2eV only. While once NiO is formed, the band is perturbed, and a new peak appears at 2eV. This new peak has been assigned to the Ni^{2-} (d^8) electrons.¹³

(II) NiO Forming Oxygen. While both the O 1s peak at 529.7eV and the Ni $2p_{3/2}$ peak at 854.3eV are observable together at 298, 373, and 423K after a considerable oxygen exposure, they appear early from the initial adsorption stage at 523K. Through a combined work of AES, LEED, and work function, Holloway *et al.*¹ have assigned these peaks to a multilayer NiO. The assignments are also supported by a number of XPS studies on single crystal Ni/O systems.

The O 1s and Ni $2p_{3/2}$ XPS spectra observed in this work coincide with the NiO spectrum obtained from thermal dissociation of $-NiO(OH)$, and accordingly, it is certain that nickel surface forms the same species of NiO, formed by thermal dissociation of $NiO(OH)$.¹⁴ The comparison of the peak intensities shows that two layers of NiO can be formed at maximum at all of the experimental temperatures except 523K, where about 3 layers can be formed.

(III) Nonstoichiometric NiO_x species. It is very reasonable to assume that some excess oxygen may adsorb on the nickel atoms of surface NiO, prior to the bulk NiO formation. This oxygen species should be less polarized than those of NiO, and accordingly the binding energy should be a little higher than those of ordinary NiO(529.7eV). The O 1s peak at 531.3eV which appears on the shoulder of the peak at 529.7eV is therefore assigned to this excess nonstoichiometric oxygen species. The increased binding energy of the Ni $2p_{3/2}$ electrons observed in this work support this assignment. It is quite probable that the surface nickel atoms with that excess oxygen adsorption will be more polarized to give a peak at the increased binding energy (856eV) over the peak at 854.3eV of the stoichiometric NiO. This shifted-up Ni $2p_{3/2}$ peak appears simultaneously with the O 1s peak at 531.3eV. Evans

*et al.*⁹ investigated the 0 ls peak intensities as a function of the radiation angle of x-ray beam, and found no intensity change at all. Thereupon, they concluded that the 0 ls species which gives a peak at 531.3eV can exist only on the surface.

Winograd *et al.*¹¹ have assumed that Ni³⁺ ion can be formed on the cation defect sites of surface NiO, and assigned the peak at 531.3eV to surface Ni₂O₃. This assignment, however, fails to account for the binding energy shift of O²⁻ ion. As regards to Ni₂O₃, the binding energy shift of Ni 2p_{3/2} should be expected, but not that of the 0 ls. In addition, there are little possibilities that the peak might be due to NiO(H) as stated in section (I) of the results.^{3,4,14}

Acknowledgements. This work was supported by a grant from the Korea Science and Engineering Foundation.

Reference

1. P. H. Holloway and J. B. Hudson, *Surf. Sci.*, **43**, 123 (1974).
2. P. H. Holloway and J. B. Hudson, *Surf. Sci.*, **43**, 141 (1974).
3. C. R. Brundle, *Surf. Sci.*, **48**, 99 (1975).
4. C. R. Brundle and A. F. Carley, *Faraday Discussion*, **60**, 51 (1975).
5. C. R. Brundle and A. F. Carley, *Chem. Phys. Letters*, **31**, 423 (1975).
6. H. Hopster and C. R. Brundle, *J. Vac. Sci. Technol.*, **16**, (2) 548 (1979).
7. T. Fleisch, N. Winograd and W. N. Delgass, *Surf. Sci.*, **78**, 141 (1978).
8. P. R. Norton, R. L. Tapping and J. W. Goodale, *Surf. Sci.*, **65**, 13 (1977).
9. S. Evans, J. Pielaszek and J. M. Thomas, *Surf. Sci.*, **56**, 644 (1976).
10. K. S. Kim and R. E. Davis, *J. Electron Spect.*, **1**, 251 (1972/1973).
11. K. S. Kim and N. Winograd, *Surf. Sci.*, **43**, 625 (1974).
12. J. H. Boo, *Thesis*(M. S) 1987.2. Sung Kyun Kwan Univ.
13. G. K. Wertheim and S. Hüfner, *Phys. Rev. Letters*, **28**, 1028(16) (1972).
14. Lee M. Moroney, Roger St C. Smart and M. Wyn Roberts, *J. Chem. Soc. Faraday Trans. I*, **79**, 1769 (1983).
15. K. H. Rieder, *Phys. Rev. B*, **27**, 6978(11) (1983).
16. M. C. Desjonqueres and F. Cyrot-Lackmann, *Surf. Sci.*, **80**, 208 (1979).
17. S. Mukherjee, V. Kumar and K. H. Bennemann, *Surf. Sci.*, **167**, L210 (1986).
18. D. E. Eastman and J. K. Cashion, *Phys. Rev. Letters*, **27**(22), 1520 (1971).
19. H. Upton and W. A. Goddard III, *Phys. Rev. Letters*, **46**, 1635 (1981).
20. P. Marcus, J. Demuth and D. Jepsen, *Surf. Sci.*, **53**, 501 (1975).

Comparisons of Stability and Spectral Response of n-Si Electrodes Modified with Polyaniline and Polypyrrole in Aqueous Solutions¹

Jin-Doo Kim and Kang-Jin Kim*

Department of Chemistry, Korea University, Seoul 136

Jung-Kyoon Chon

Department of Chemistry, Han Kuk University of Foreign Studies, Seoul 131. Received April 17, 1987

Modification of n-Si electrodes coated by photogalvanostatically with polyaniline and polypyrrole in aqueous solutions considerably enhanced the stability and the spectral response of the photoelectrodes. A polypyrrole coated electrode incorporated with redox couple Fe(CN)₆³⁻/Fe(CN)₆⁴⁻ yielded a photocurrent density of 400 μA/cm² for about 120 hours. Broad spectral responses over 300-850 nm were observed for both polymer coated electrodes of which polypyrrole coated one showed better current conversion efficiency.

Introduction

Recently the use of n-type semiconductors as the photoanodes to the electrolysis of water has aroused a great deal of interest which stems from the expectation that the light-stimulated electrode process may offer fairly good means of converting solar energy to electrical or chemical energy.²⁻⁵ To achieve an efficient utilization of the immense solar energy, it is desirable for an semiconductor electrode to possess the small band gap among other things.⁶ Theoretical calculations show that the optimum band gap of a phototelec-

trode for the electrolysis of water is 1.3 ± 0.3 eV which corresponds to the absorption of light of 1000 ± 250 nm.^{3,7} An n-Si semiconductor has a favorable band gap of 1.14 eV and it is one of the cheapest semiconductors, well-understood in the solid state physics, and most nearly perfect crystalline material available. Unfortunately, an electrode of small band gap, including n-Si, has a drawback of corrosion in aqueous electrolyte solutions under illumination. The photogenerated holes not only corrode the semiconductor itself, but may introduce surface states where the recombination reactions with electrons convert the absorbed energy into